

# Single-Electron Tunneling Spectroscopy in Nanoparticles

Hongki Min\*

Department of Physics, The University of Texas at Austin, Austin TX 78712

(Dated: May 6, 2005)

The discrete excitation spectrum of an individual metallic nanoparticle can be measured by the technique of single-electron tunneling spectroscopy. In this report, recent experimental work on ultrasmall metallic grains are reviewed focusing on the influence of the spin-orbit scattering on the discrete spectrum in nonmagnetic Al and ferromagnetic Co nanoparticles.

## I. INTRODUCTION

One of the fundamental features of quantum mechanics is that the energy spectrum of particles confined to a small system is discrete or quantized and the typical energy level spacing increases as the system size decreases. The discrete spectra in these condensed matter systems can provide a tool for understanding the interactions which influence electronic structure, uncovering effects that are not clearly visible if the individual quantum levels in the system cannot be resolved. However, in condensed matter system, it is not easy to see the discrete energy spectrum of an individual sample because system sizes are typically so large that discrete energies could not be resolved on the energy scale set by the temperature.

In 1990s [1, 2], the development of *single-electron tunneling spectroscopy* made it possible to resolve discrete energy levels even for small metallic grains which usually have much higher density of states than semiconductors, thus requiring much smaller sample size. It relies on the Coulomb blockade effect of a nanoparticle connected to a circuit by tunneling barriers. The tunneling conductance shows a number of peaks as a function of bias voltage, interpreted as transitions between quantum levels of the particle.

In this report, the basic idea of the single-electron tunneling spectroscopy will be summarized and then recent experiments on nonmagnetic and ferromagnetic nanoparticles will be discussed. Finally, remaining problems will be discussed.

## II. SINGLE-ELECTRON TUNNELING SPECTROSCOPY

### A. Experimental Setup

A schematic cross section of the device geometry is shown in this figure. The devices are fabricated as follows. Using electron-beam lithography and etching technique, silicon nitride membrane containing a bowl-shaped hole is fabricated. Then the gate electrode is formed by evaporating Al onto the flat side of the membrane. Next,

an aluminum electrode is formed which fills the bowl-shaped side of the membrane. Then a layer of nanoparticles is created by depositing Al onto the lower side of the device. Due to surface tension, Al nanoparticles gather to form small particles less than 10 nm in diameter. Devices in which tunneling occurs via a single nanoparticle joining the two leads are selected based on the measurement of a Coulomb staircase.

In the single electron tunneling spectroscopy, applying a bias voltage between the two leads causes a tunnel current to flow between the leads through the grain. In addition, the grain is also coupled to a gate so that the tunneling current can be influenced by changing the gate voltage, which tunes the electrostatic potential on the grain and thereby also its average number of electrons. Therefore, the resulting device shown in Fig.1 has a structure of *single electron transistor*.

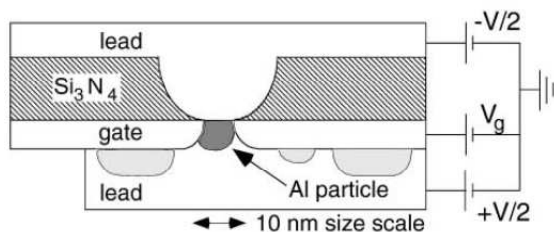


FIG. 1: Schematic cross section of the single-electron transistor [2].

### B. $I$ - $V$ Measurements

In an experiment the measured quantity is the current  $I$  through the device as a function of the voltage difference  $V$ . When  $V$  is varied on a large scale of tens of mV, the  $I$ - $V$  curve shows a steplike behavior. The flatness around zero voltage occurs because no current can flow through the grain until it overcomes the charging energy. This phenomenon is called the *Coulomb blockade* effect.

When  $V$  is varied on the much smaller scale of a few mV around the threshold of the Coulomb blockade regime and the temperature is sufficiently low, the  $I$ - $V$  curves have a step-like substructure (Fig.3). As  $V$  is increased above the threshold charging energy, an additional resonant tunneling occurs whenever the Fermi level

\*Electronic address: hongki@physics.utexas.edu

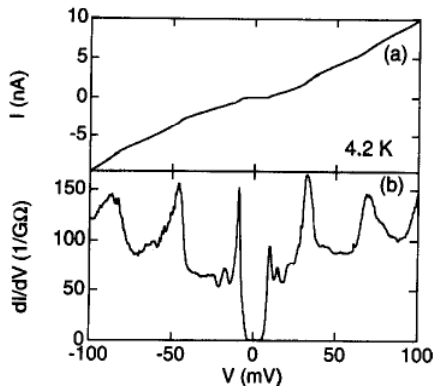


FIG. 2:  $I$ - $V$  curve of the single-electron transistor at 4.2 K showing the Coulomb blockade region with  $I=0$  near  $V=0$  [3].

in one of the two leads match the discrete energy states of the particle. This means that the individual quantum states in the grain become accessible to tunneling.

Note that the energy scales of the charging energy and the mean level spacing are quite different. Typical charging energy is roughly ranging from 5 ~ 50 meV, whereas mean level spacing typically  $0.02 < d < 0.3$  meV which is much smaller than the charging energy but much larger than the thermal energy set by temperature (around  $T \sim 30$  mK). Since the two scales differ by at least an order of magnitude, it is easy to separate their contributions in the low-temperature  $I$ - $V$  curves of the devices.

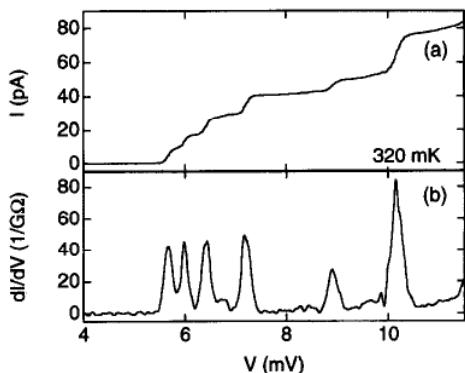


FIG. 3:  $I$ - $V$  curve of the single-electron transistor at 320 mK showing onset of current steps at voltages above the Coulomb blockade where individual quantum states in the grain become accessible to tunneling [3].

### III. NONMAGNETIC NANOPARTICLES

#### A. Experimental Results

The nanoparticles in the tunneling experiment is normally pure Al and the effective  $g$  factor is the same with 2 which is the free electron  $g$  factor. The energy spectra shows linear dependence on the applied magnetic field. However, for several of the normal-state grains in the experiments, the magnetic-field dependence of the excitation spectra showed marked deviations from the simple behavior:  $g$  factors differing from 2 were measured and deviations from linear  $H$ -dependence in the form of avoided level crossings were observed.

The nanoparticles in the tunneling experiment is normally pure Al. In some of the devices however, the Al evaporation for the particles was interrupted and a thin layer of gold was deposited corresponding roughly to a 4 % of doping inside the nanoparticle. These unintended defect or impurity can be identified as the source of the spin-orbit scattering.

Tunneling spectra of the discrete energy levels are shown in Fig.(4) at different values of the applied magnetic field for an Al particle which presumably containing doped Au. The peaks in Fig.(4) have many features qualitatively similar to those in pure Al. As the applied magnetic field parallel to the silicon nitride membrane is increased, each peak splits linearly into two at low magnetic field.

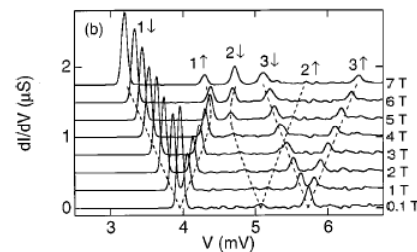


FIG. 4: Tunneling spectrum of discrete state resonances in the sample, for a range of applied magnetic fields at  $T=55$  mK. [4].

However, there are several features different from pure Al particles. First, let's define an effective  $g$  factor such that the energy splitting between Zeeman-split states is  $\Delta E = g_{\text{eff}} \mu_B H$  to linear order of in  $H$ . In normally pure Al samples,  $g_{\text{eff}} = 2 \pm 0.05$ , which is as expected, because spin-orbit scattering is negligible in pure Al, and the free-electron  $g$  factor should apply. In the sample in question,  $g_{\text{eff}}$  is significantly less, and it varies from peak to peak,  $g_{\text{eff}} = 1.84 \pm 0.03, 1.68 \pm 0.08$  and  $1.76 \pm 0.05$  for the three resonances in Fig.(5).

Secondly, avoided level crossings were observed. In pure Al particles with  $g$  factors approximately 2, any departures from linear Zeeman splittings were not observed. For a sample without spin-orbit scattering, this must be the case, because there is no coupling between spin-up

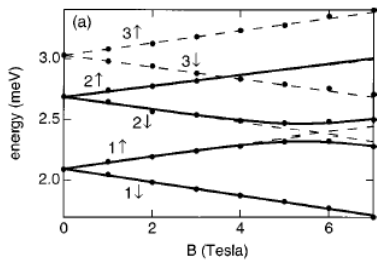


FIG. 5: Energies of the discrete electronic states within the nanoparticle of Fig.(4). [4].

and spin-down states in the Hamiltonian. In contrast, the Zeeman splittings of levels  $1_\uparrow$  and  $2_\downarrow$  in Fig.(5) show a clear departure from the linear behavior and the upward-trending  $1_\uparrow$  level undergoes an avoided crossing with the down-trending  $2_\downarrow$ .

### B. Simple Model

As mentioned in the previous section, the presence of spin-orbit scattering within an Al nanoparticle affects measurements of the discrete energy levels by reducing the effective  $g$  factor below the free-electron value 2 and causing avoided crossings as a function of magnetic field between predominantly spin-up and predominantly spin-down levels.

These features can be understood by considering Hamiltonian in the presence of spin-orbit scattering. Let's write the Hamiltonian in zero magnetic field as

$$H = H_0 + H_{SO} \quad (1)$$

where  $H_0$  describes all the spin-independent interactions and  $H_{SO}$  contains the terms that couple spin-up states to spin-down states. Then, performing perturbation theory to the lowest order in  $H_{SO}$ , the eigenstate  $n$  with predominantly spin up is given by

$$|n_\uparrow\rangle \approx |n_\uparrow^{(0)}\rangle + \sum_{m \neq n} \frac{|m_\downarrow^{(0)}\rangle \langle m_\downarrow^{(0)} | H_{SO} | n_\uparrow^{(0)} \rangle}{E_n - E_m} \quad (2)$$

and the effective  $g$  factor for the eigenstate  $n$  can be written as

$$g_{eff,n} = g_0 \frac{\langle n_\uparrow | \sigma_z | n_\uparrow \rangle}{\langle n_\uparrow | n_\uparrow \rangle} \quad (3)$$

$$\approx g_0 \left( 1 - 2 \sum_{m \neq n} \frac{|\langle m_\downarrow^{(0)} | H_{SO} | n_\uparrow^{(0)} \rangle|^2}{(E_n - E_m)^2} \right)$$

Therefore,  $g_{eff}$  is reduced below the free-electron value  $g_0 = 2$  by an amount determined by the spin-orbit matrix elements which couple the state  $n$  to other states with opposite spin. Because the energy eigenstates are

no longer purely spin up or spin down in the presence of spin-orbit interactions, they respond more weakly to an applied magnetic field than pure-spin states, resulting in the reduced  $g$  factor.

Note that for very small systems, the mean level spacing become larger than the typical spin-orbit matrix element so it is legitimate to treat the spin-orbit interaction as a weak perturbation. With larger systems, the energy denominators decrease and eventually lead to the breakdown of perturbation theory. However in the bulk limit, it can be shown that the relevant energy denominators are of the order of the bandwidth thus the effect of spin-orbit interactions will be small though the mean level spacing becomes extremely small. Indeed bulk  $g$ -factors, in general deviate very little from the free electron  $g$  factor. Therefore, the spin-orbit effect is expected to have its strongest impact in the mesoscopic regime with mean level spacing comparable to or smaller than typical spin-orbit matrix elements.

In order to analyze the avoided level crossing in Fig.(5), let's consider only the lowest four levels and construct the effective truncated Hamiltonian. To this end, the eigenstates  $n = 1, 2$  in eq.(2) can be used as a basis which are defined in the  $H = 0$  limit with spin-orbit correction included. It is now straightforward to solve this truncated problem explicitly and to find the energies as a function of the applied magnetic field.

## IV. FERROMAGNETIC NANOPARTICLES

### A. Experimental Setup

The fabrication for ferromagnetic Co particles is similar to that of nonmagnetic Al particles and schematic cross section is shown in Fig.6. The top Al electrode is deposited first so as to fill a bowl etched through a  $\text{Si}_3\text{Ni}_4$  membrane with hole radius  $< 5$  nm, and then a tunnel barrier is formed by oxidizing Al. The Co nanoparticles are obtained by evaporation at room temperature of a Co layer. Surface tension causes the Co to form electrically separate particles in the range of 1-4 nm diameter.

### B. Experimental Results

Fig.7 shows the tunneling spectra at the onset of conduction for the first Coulomb threshold for three samples. Similarly as nonmagnetic case shown in Fig.3, the tunneling spectra for Co nanoparticles show well-resolved peaks due to tunneling via discrete electron levels within each particle.

However, the tunneling spectra for ferromagnetic nanoparticles are different in several interesting ways from nonmagnetic nanoparticles. First, energy levels are coupled to the direction of the particle's total magnetic moment, such that the levels shift as the moment is re-oriented. Second, the magnetic dependence of the ener-

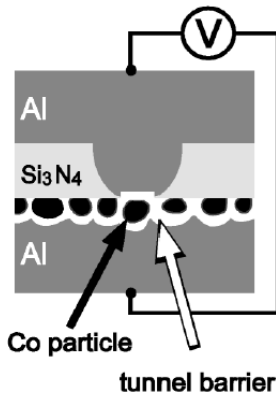


FIG. 6: Schematic cross section of the single-electron transistor [5].

gies show the same sign of the slope. Third, the energy spacing of the resonances is smaller than expected in an independent-electron model, suggesting the importance of low-energy many-body spin excitation. Let's consider each point in detail.

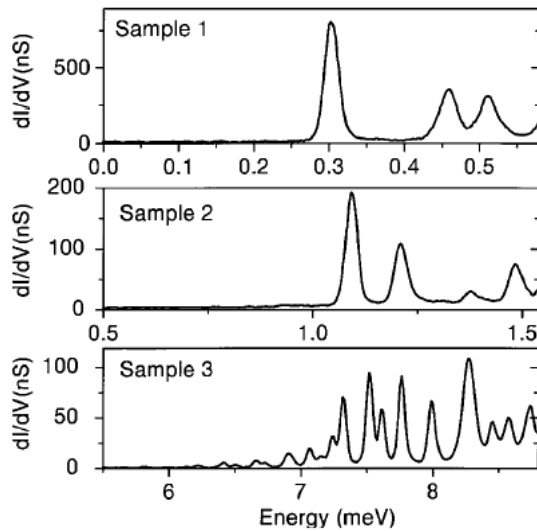


FIG. 7: Tunneling spectra of three different samples at  $T = 20$  mK and  $H=1$  T.  $H$  is parallel to  $\text{Si}_3\text{Ni}_4$  membrane [5].

Unlike nonmagnetic particles where the energy levels have a simple linear dependence on  $H$  due to the Zeeman energy, the levels in Co have a strong nonlinear dependence on  $H$  for small  $H$ . Fig.8 shows the energy of the first three tunneling resonances of sample 1 as an external magnetic field  $H$  is swept from negative to positive values and back again along the direction oriented 45° from the easy axis. Starting from  $-0.45$  T, the tunneling energies shift in a continuous manner and the magnetic moment of the particle relaxes toward its easy axis. Note that at  $H = 0.23$  T, all the levels show sudden jumps. We can interpret this jump due to the reversal of the magnetization in a single domain Co nanoparticle.

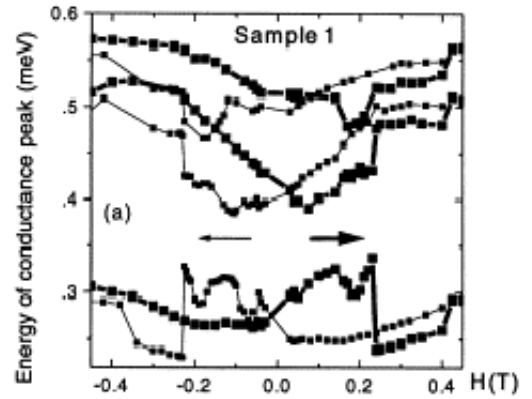


FIG. 8: Magnetic-field dependence of the tunneling spectra of several Co grains. Hysteresis shows the dependence of tunneling energies on  $H$  at  $T = 20$  mK for sample 1 [5].

The energy shifts with  $H$  are hysteretic with respect to the direction of the field sweep. These curves indicate a significant coupling between the level energies and the orientation of the magnetic moment of the nanoparticle. Therefore, the quantum states in a ferromagnetic nanoparticle are not all described by the same anisotropy-energy function that governs the ground state, but anisotropy varies from state to state.

At larger values of  $H$ , all the energy levels increase as a function of  $H$  with slopes that correspond to effective  $g_{\text{eff}}$  factors. Fig.9 shows that  $g_{\text{eff}}$  factors vary between 0.8 to 1.9 and fluctuate quite strongly from level to level. Similarly as the nonmagnetic particles, level dependent reduced  $g$  factors can be understood due to the effect of the spin-orbit scattering.

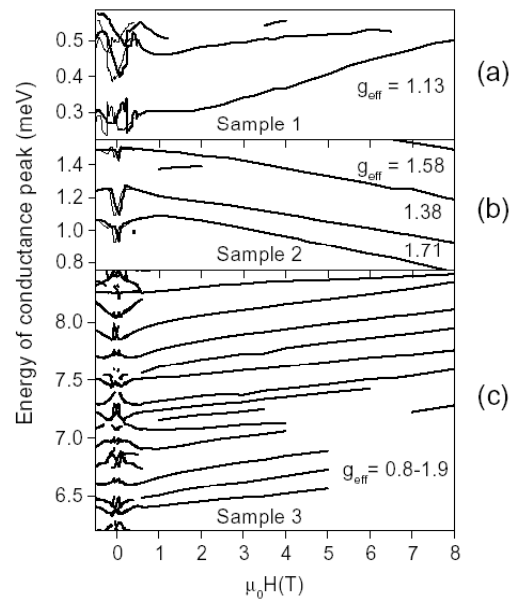


FIG. 9: Tunneling spectra of three different samples at  $T = 20$  mK and  $H=1$  T.  $H$  is parallel to  $\text{Si}_3\text{Ni}_4$  membrane [5].

Also we can observe that all measurable transition energies within a given sample have the same sign of the slope as a function of  $H$ . This is different from results in Al for which Zeeman spin splitting of each orbital state gives rise to lines with upward and downward slopes with comparable conductance amplitudes and with a degeneracy at  $H=0$ . Note that Co is not fully spin polarized ( $P \approx 30\%$ ) so both slopes would be expected to occur even if in unequal numbers and with different amplitudes.

Finally, let's consider the measured density of tunneling resonances shown in Fig.7. The energy spacing between tunneling peaks is somewhat less than 0.2 meV, much smaller than the value expected from the mean level spacing  $d$  for noninteracting electrons, between 0.75 and 40 meV. One possible explanation is that electron excitations within a Co particle may include low-energy spin waves in addition to the electron-hole excitations due to the spin-orbit coupling.

### C. Simple Model

The hysteretic behavior can be understood qualitatively in terms of a simple model Hamiltonian.

$$H = -g_{\text{eff}}\mu_B\vec{H} \cdot \vec{S} - K_m\mu_B S_z^2 / \sqrt{S(S+1)} \quad (4)$$

where  $K_m$  is an anisotropy energy per unit magnetic moment.

It includes Zeeman energy with the total electronic spin  $\vec{S}$  and an easy-axis anisotropy energy in the  $z$  direction. We assume that the Zeeman and anisotropy energies are sufficiently weak relative to the exchange splitting between different spin multiplets that the magnitude  $S$  in the ground state remains constant as  $H$  is varied. Then by diagonalizing the model Hamiltonian for a grain with  $N$  or  $N \pm 1$  electrons (and spin  $S$  or  $S \pm 1/2$ ), the tunneling spectrum can be calculated for spin increasing and decreasing transitions, giving the qualitative agreement with Fig.8.

However, this model fails to capture an important detail. The observed transitions shift as a function of magnetic field with the same sign of the slope is still a mystery. In addition, the systematic explanation for the smaller level spacing is still missing. A possible candidate is the contributions of low-energy collective spin-wave excitations, which can be estimated as  $\approx 0.1$  meV and is comparable to the observed energy level spacing.

### Acknowledgments

I wish to thank Prof. Qian Niu for his interesting lectures with physical insight in the nanostructure class.

- 
- [1] C. Black, D. Ralph, and M. Tinkham, Phys. Rev. Lett. **76**, 688 (1996).
  - [2] D. Ralph, C. Black, and M. Tinkham, Phys. Rev. Lett. **78**, 4087 (1997).
  - [3] M. Tinkham, Am. J. Phys. **64**(3), 343 (1996).
  - [4] D. Salinas, S. Gueron, D. Ralph, C. Black, and M. Tinkham, PRB. **60**, 6137 (1999).
  - [5] S. Gueron, M. M. Deshmukh, E. Myers, and D. Ralph, Phys. Rev. Lett. **83**, 4148 (1999).